Journal of Mathematical Modeling
Vol. 13, No. 1, 2025, pp. 85-103. Research Article

JMM

Non-standard finite-difference scheme for singularly perturbed parabolic convection-diffusion problem with boundary turning points

Yimesgen Mehari Kebede*, Awoke Andargie Tiruneh, Endalew Getnet Tsega

Department of Mathematics, College of Science, Bahir Dar University, Bahir Dar, Ethiopia
Email(s): yimesgen2004@gmail.com, awoke248@yahoo.com, endalebdumath2016@gmail.com

Abstract. This paper presents a numerical method for solving singularly perturbed parabolic convection-diffusion problems with boundary turning points. As the perturbation parameter ε approaches zero, the solution shows rapid changes on the left side of the spatial domain, forming a small boundary layer. The classical finite difference methods on uniform meshes fail to capture these oscillations without using a large number of mesh points. To solve this, we use the implicit Euler method for time discretization and a non-standard finite difference method in space. The method satisfies stability, the discrete minimum principle, and ε-uniform convergence. Error estimates show that the proposed method is first-order convergence in time and space. The order of convergence is improved by applying the Richardson extrapolation method. Two model examples are provided to show the scheme's applicability. It demonstrates that the numerical results are in agreement with the theoretical findings.

Keywords: Singularly perturbed, boundary turning points, non-standard finite difference scheme, uniform convergence, Richardson extrapolation.
AMS Subject Classification 2010: 65M06, 65M12, 65M15.

1 Introduction

Singularly perturbed parabolic convection-diffusion equations are partial differential equations (PDEs) that combines elements of the convection and diffusion with a small parameter ε $(0 < \varepsilon \ll 1)$ multiplying the highest order derivative term in the PDEs that leads to a stiff behavior in a certain region of the solution domain. The behavior (location) of such region depends on the sign of the coefficient of the convection term which is negative, positive or zero. If the coefficient of convective term is zero at one of the boundary of the domain, then the problem is called singularly perturbed problem (SPP) with boundary turning point. This problem arises in the processes modeling of convective transport of a diffusing

*Corresponding author
Received: 23 June 2024 / Revised: 12 August 2024 / Accepted: 12 September 2024
DOI: 10.22124/jmm.2024.27766.2445

substance (heat, matter) for the case in which the rate of flow from one of the boundaries is proportional to the distance from the boundary [20]. The model problems of this paper corresponds to the flow directed outward the left boundary of the domain with a stop of the flow on this boundary. This class of problems also models the heat flow and mass transport near oceanic rises [3] and appears in the modeling of thermal boundary layers in laminar flow [23]. The problem in [3] is a single boundary turning point problem because of the assumption that the velocity distribution is linear. If one allows for higher orders of velocity distribution, then the boundary turning point becomes multiple. Multiple (second-order) boundary turning point problems are given in ([23], Chapter 12), and drift-diffusion equation of semiconductor device [17]. Finding the solution of these type of problems are more challenging than the non turning point problems and attracted the attention of various scholars [2, 7, 8, 10–13, 16, 21, 24]. Kumari et al. [7] have considered SPPs including a boundary turning point of multiplicity greater than or equal to one. They proposed a numerical scheme comprising of the Crank-Nicolson in temporal direction and upwind scheme on Shishkin mesh in the spatial direction. Swati et al. [24] proposed a numerical scheme comprising an implicit finite difference method for time discretization on a uniform mesh and a hybrid scheme for spatial discretization on a generalized Shishkin mesh. Sahoo and Gupta [10] had developed a first-order ε uniform convergent scheme using implicit Euler method on uniform mesh in time and a simple upwind scheme on piece wise uniform mesh in space. One can see [15, 19] for more details of existing literature on asymptotic analysis and numerical methods for the turning point problems. As we observed, the developed schemes used the fitted mesh method for solving the problem of type in [7], which requires prior knowledge about the location and width of the boundary layer. Sometimes, this requirement is difficult to be satisfied.

Non-standard finite difference methods (NSFDMs), nowadays, are playing a crucial role in the development of reliable numerical methods to solve SPPs. These NSFDMs are designed using the exact finite difference scheme, and the denominator function should be complicated. There are no general guidelines for doing so, but the advantage of this method is that it is straightforward to implement and extendable to higher-dimensional problems. However, the following important rules have been discovered by Mickens [14].

- **Rule 1:** The orders of the discrete derivative should be equal to the orders of the corresponding derivatives appearing in the differential equations.
- **Rule 2:** Denominator functions for the discrete derivatives must, in general, be expressed in terms of more complicated functions of the step-sizes than those conventionally used.
- **Rule 3:** Nonlinear terms should, in general, be replaced by non local discrete representations.
- **Rule 4:** Special conditions that hold for the solutions of the differential equations should also hold for the solutions of the finite difference scheme.
- **Rule 5:** The discrete schemes should not produce extraneous or spurious solutions.

Important physical features of the solutions to the associated problem can be numerically preserved through the development and application of NSFD methods using these rules [1, 4, 9, 18, 22, 25, 26]. The purpose of this paper is to construct and analyse a numerical scheme which presents relatively rapid convergence and accuracy for solving the problem considered in [7]. We proposed a parameter uniformly convergent numerical scheme using implicit Euler method in time and a non-standard finite difference

method in space with uniform meshes to solve the problem of concern. Theoretically, we showed that the proposed scheme has accuracy $O(M^{-2}+N^{-2})$, where N and M are the number of mesh intervals in space and time respectively.

Notation: Throughout this article, C denotes a generic positive constant independent of ε and the mesh parameters. All the functions defined on the domain $W = \ominus \times (0,T]$, $\ominus = (0,1)$, $T > 0$ are measured in maximum norm as,

$$||g||_{\bar{W}} = \sup_{x \in \bar{W}} |g(x)|, \text{ where } \bar{W} = [0,1] \times [0,T].$$

The boundary of the domain is $\partial W = \bar{W} \backslash W = \Gamma_l \cup \Gamma_b \cup \Gamma_r$, where

$$\begin{cases} \Gamma_l = \{x = 0 \mid 0 \le t \le T\}, \\ \Gamma_b = \{t = 0 \mid 0 \le x \le 1\}, \\ \Gamma_r = \{x = 1 \mid 0 \le t \le T\}. \end{cases}$$

2 Properties of continuous problem

Consider the following singularly perturbed parabolic convection-diffusion initial-boundary value problem on $W = \ominus \times (0,T]$, $\ominus = (0,1)$, $T > 0$ with smooth boundary $\partial W = \bar{W} \backslash W = \Gamma_l \cup \Gamma_b \cup \Gamma_r$:

$$\begin{cases} \mathscr{L}_\varepsilon u(x,t) = f(x,t), \quad (x,t) \in W, \\ u(x,0) = u_0(x), \quad x \in \bar{\ominus}, \\ u(0,t) = \phi(t), \;\; u(1,t) = \psi(t), \quad t \in (0,T], \end{cases} \tag{1}$$

where

$$\begin{cases} \mathscr{L}_\varepsilon u(x,t) \equiv \varepsilon u_{xx} + a(x,t)u_x - b(x,t)u(x,t) - u_t(x,t), \\ a(x,t) = a_0(x,t)x^p, \;\; p \ge 1, \\ a_0(x,t) \ge \alpha > 0, \;\; b(x,t) \ge \beta > 0 \;\text{ on }\; \bar{W}. \end{cases} \tag{2}$$

such that $a_0(x,t), b(x,t), \psi, \phi$ and $f(x,t)$ are smooth and bounded in $\bar{W}$. From equation 2 if $p \neq 1$, then, problem (1) is called multiple a boundary turning point problem. Otherwise, it is a simple boundary turning point problem. Setting $\varepsilon = 0$ in the equations (1)-(2) gives the reduced problem

$$a(x,t)(v_0(x,t))_x - b(x,t)v_0(x,t) - (v_0(x,t))_t = f(x,t),$$

which is first order hyperbolic PDE along with initial and boundary conditions

$$\begin{cases} u(x,0) = u_0(x), \quad x \in \bar{\ominus}, \\ u(0,t) = \phi(t), \quad u(1,t) = \psi(t), \quad t \in (0,T]. \end{cases}$$

Since only one boundary condition is needed to solve this reduced problem, one boundary condition will be underutilized, resulting boundary layer in that neighbourhood. The convective term is positive over the domain W. The boundary layer will therefore be found close to $x = 0$. According to Kumari et al. (2023), the layer's width is expressed as $O(\sqrt{\varepsilon})$.

Let $u_0(x) \in C^2[0,1]$, $\psi, \phi \in C^1[0,T]$. We impose the compatibility conditions

$$u_0(0) = \phi(0), \;\; u_0(1) = \psi(1), \tag{3}$$

and

$$\begin{cases} \varepsilon \frac{\partial^2 u_0(0)}{\partial x^2} + a(0,0)\frac{\partial u_0(0)}{\partial x} - b(0,0)u_0(0) - \frac{\partial \phi(0)}{\partial t} = f(0,0), \\ \varepsilon \frac{\partial^2 u_0(1)}{\partial x^2} + a(1,0)\frac{\partial u_0(1)}{\partial x} - b(1,0)u_0(1) - \frac{\partial \phi(1)}{\partial t} = f(1,0), \end{cases} \tag{4}$$

so that the data matches at the two corners (0,0) and (1,0). These assumptions ensure that there exists a constant C such that $\forall (x,t) \in \bar{W}$

$$u(x,0) - Ct \leq u(x,t) \leq Ct + u(x,0), \tag{5}$$

$$u(0,t) - C(1-x) \leq u(x,t) \leq C(1-x) + u(0,t). \tag{6}$$

Lemma 1. *The bound on the solution $u(x,t)$ of the continuous problem (1) is given by $|u(x,t)| \leq C$.*

Proof. From the equation (5) we have

$$|u(x,t) - u(x,0)| = |u(x,t) - u_0(x)| \leq Ct.$$

Now,

$$|u(x,t)| - |u_0(x)| \leq |u(x,t) - u_0(x)| \leq Ct,$$

which implies that

$$|u(x,t)| \leq Ct + |u_0(x)|, \;\; \forall (x,t) \in \bar{W}.$$

Since $t \in [0,T]$ and $u_0(x)$ is bounded, it gives $|u(x,t)| \leq C$. □

Lemma 2. ***(The Continuous Minimum Principle)*** *Let $F(x,t)$ be a sufficiently smooth function defined on W which satisfies $F(x,t) \geq 0, \forall (x,t) \in \partial W$ and $\mathscr{L}_\varepsilon F(x,t) \leq 0, \;\; \forall (x,t) \in W$. Then $F(x,t) \geq 0, \;\; \forall (x,t) \in \bar{W}$.*

Proof. Let the point $(y,z) \in \bar{W}$ and $F(y,z) = \min\limits_{(x,t)\in \bar{W}} F(x,t) < 0$. Since $F(x,t) \geq 0, \;\; \forall (x,t) \in \partial W$, we have $(y,z) \notin \partial W$. The inequality $F(y,z) = \min\limits_{(x,t)\in \bar{W}} F(x,t) < 0$ implies that $\frac{\partial F(y,z)}{\partial t} = 0$, $\frac{\partial F(y,z)}{\partial x} = 0$ and $\frac{\partial F(y,z)}{\partial x} \geq 0$. Giving that

$$\mathscr{L}_\varepsilon F(y,z) = (\varepsilon \frac{\partial^2 F}{\partial x^2} + a\frac{\partial F}{\partial x} - bF - \frac{\partial F}{\partial t})(y,z) > 0,$$

which contradict the assumption that $\mathscr{L}_\varepsilon F(x,t) \leq 0, \forall (x,t) \in W$. Therefore, $F(x,t) \geq 0, \;\; \forall (x,t) \in \bar{W}$. □

Lemma 3 (Stability Estimate). *Suppose $u(x,t)$ be the solution of (1), then it satisfies*

$$||u(x,t)||_{\bar{W}} \leq ||u(x,t)||_{\partial W} + \frac{||f(x,t)||_{\bar{W}}}{\beta}.$$

Proof. Consider the barrier functions

$$\eth^{\pm}(x,t) = ||u(x,t)||_{\partial W} + \frac{||f(x,t)||_{\bar{W}}}{\beta} \pm u(x,t).$$

On the boundary points

$$\eth^{\pm}(0,t) = ||u(0,t)||_{\partial W} + \frac{||f(0,t)||_{\bar{W}}}{\beta} \pm u(0,t) \geq 0,$$
$$\eth^{\pm}(1,t) = ||u(1,t)||_{\partial W} + \frac{||f(1,t)||_{\bar{W}}}{\beta} \pm u(1,t) \geq 0,$$

and in the interior points,

$$\begin{aligned}\mathscr{L}_{\varepsilon}\eth^{\pm}(x,t) &= -b(x,t)[||u(x,t)||_{\partial W} + \frac{||f(x,t)||_{\bar{W}}}{\beta}] \pm \mathscr{L}_{\varepsilon}u(x,t) \\ &\leq -\beta[||u(x,t)||_{\partial W} + \frac{||f(x,t)||_{\bar{W}}}{\beta}] \pm f(x,t) \leq 0.\end{aligned}$$

Using Lemma 2, $\eth^{\pm}(x,t) \geq 0, \ \ \forall (x,t) \in \bar{W}$. This implies that $||u(x,t)||_{\bar{W}} \leq ||u(x,t)||_{\partial W} + \frac{||f(x,t)||_{\bar{W}}}{\beta}$. □

Theorem 1. *Under the compatibility conditions* (3) *and* (4)*, problem* (1) *satisfies the following bounds for* $0 \leq i+3j \leq 4$

$$\left|\frac{\partial^{i+j}}{\partial x^i \partial t^j}u(x,t)\right| \leq C(1+\varepsilon^{-i/2}exp(-x\sqrt{\frac{\beta}{\varepsilon}})), \ \ (x,t) \in \bar{W}.$$

Proof. For a fixed $i = 0$ and on the boundaries $x = 0$ and $x = 1$ of $\bar{\ominus}$ we have $u = 0$, therefore $u_t = 0$. On the boundaries of $t = 0$, we have $u = 0$ therefore $u_x = 0$ and $u_{xx} = 0$. Hence from (1) we have $u_t(x,0) = f(x,0)$. Since f is bounded, we can choose large K_1 such that $|u_t| \leq K_1$.
Now, consider the operator $\mathscr{L}_{\varepsilon}u(x,t) \equiv \varepsilon u_{xx} + a(x,t)u_x - b(x,t)u(x,t) - u_t(x,t) = f$, and differentiating with respect to t we have,

$$\mathscr{L}_{\varepsilon}u_t(x,t) \equiv (\varepsilon u_{xx} + a(x,t)u_x - b(x,t)u(x,t) - u_t(x,t))_t = f_t.$$

This implies $\mathscr{L}_{\varepsilon}u_t(x,t) \leq K_2$, since f is smooth. Since the operator $\mathscr{L}_{\varepsilon}$ satisfies the minimum principle on $\bar{\ominus}$, we can conclude by the above estimate $|u_t| \leq C$ on $\bar{\ominus}$. Thus, $|u_t| \leq C\exp(-x\sqrt{\frac{\alpha}{\varepsilon}})$ for $0 \leq x \leq 1$.

To bound the derivatives of the solution in the spatial domain, consider the cases for a fixed $j = 0$.

For $i = 0$, from Lemma 1 we have $|u| \leq C$. For $i = 1$, by using arguments in [6], construct the neighbourhood of $I = (0, \sqrt{\varepsilon}), \ \ \forall r \in I$. For some $r^* \in I$ by mean value theorem, we have

$$u_x(r^*) = \frac{u(\sqrt{\varepsilon}) - u(0)}{\sqrt{\varepsilon}}.$$

It implies that

$$|u_x(r^*)| = \varepsilon^{-1/2}\left|u(\sqrt{\varepsilon}) - u(0)\right| \leq C\varepsilon^{-1/2}||u||. \tag{7}$$

Now, Eq. (1) can be rewritten as

$$\mathscr{L}_{\varepsilon}u(x,t) \equiv \varepsilon u_{xx} + (au)_x - (a_x + b)u - u_t = f,$$

which implies

$$\varepsilon u_{xx} + (au)_x = f + (a_x + b)u + u_t.$$

So

$$\int_{r^*}^{r} (\varepsilon u_{xx} + (au)_x)dx = \int_{r^*}^{r} (f + (a_x + b)u + u_t)dx,$$

which gives

$$(\varepsilon u_x + (au))\Big|_{r^*}^{r} = \int_{r^*}^{r} (f + (a_x + b)u + u_t)dx \leq C \int_{r^*}^{r} (||f|| + ||u|| + ||u_t||)dx \leq C\varepsilon^{1/2}.$$

Now,

$$\varepsilon u_x(r,t) + a(r,t)u(r,t) \leq \varepsilon u_x(r^*,t) + a(r^*,t)u(r^*,t) + C\varepsilon^{1/2}.$$

Since for $r \in (0, \sqrt{\varepsilon})$, $|a(r,t)| = \left|a_0(r,t)r^k\right| \leq C\varepsilon^{k/2}$, $k = 1,2,3,\ldots$ and using Eq. (7), we have the following

$$\begin{aligned} |u_x(r,t) \leq & |a(r^*,t)u_x(r^*,t)| + |\frac{a(r,t)u(r,t)}{\varepsilon}| + |\frac{a(r^*,t)u(r^*,t)}{\varepsilon}| + C\varepsilon^{-1/2} \\ \leq & c_1\varepsilon^{-1/2} + c_2\varepsilon^{k/2-1} + c_3\varepsilon^{k/2-1} + C\varepsilon^{-1/2} \\ \leq & C_4\varepsilon^{-1/2} \leq C(1 + \varepsilon^{-1/2}\exp(-x\sqrt{\frac{\beta}{\varepsilon}})). \end{aligned}$$

For $i = 1$, the process is done. In the same manner, bound can be established for the remaining higher order derivatives using repeated differentiation. □

3 Formulation of numerical scheme

To obtain the full discrete scheme, first discretize the time variable using implicit Euler method with uniform mesh and then apply non-standard finite difference technique [14] in space variable.

3.1 Temporal semi-discretization

We discretize the time domain [0,T] using uniform mesh with length k by

$$\bar{W}_t^M = \left\{ t_j = jk, \quad j = 0,1,\ldots,M, \quad k = \frac{T}{M} \right\}, \tag{8}$$

where M is the number of mesh intervals in the temporal discretization. Now, using implicit Euler method, we have

$$\begin{cases} \varepsilon u_{xx}^{j+1}(x) + a^{j+1}(x)u_x^{j+1}(x) - b^{j+1}(x)u^{j+1}(x) - D_t^- u^{j+1}(x) = f^{j+1}(x), \\ u(0,t_{j+1}) = \phi(t_{j+1}), u(1,t_{j+1}) = \psi(t_{j+1}), u(x,0) = u_0(x), \\ x \in \ominus, \ 0 \leq j \leq M-1, \end{cases} \tag{9}$$

where

$$D_t^- u^{j+1}(x) = \frac{u^{j+1}(x) - u^j(x)}{k}.$$

The semi-discretized problem (9) can be rewritten as

$$\begin{cases} \hat{\mathscr{L}}_\varepsilon u^{j+1}(x) = f^{j+1}(x) - \frac{u^j(x)}{k}, \\ u(0,t_{j+1}) = \phi(t_{j+1}), u(1,t_{j+1}) = \psi(t_{j+1}), u(x,0) = u_0(x), \\ x \in \ominus, \;\; 0 \le j \le M-1, \end{cases} \tag{10}$$

where

$$\hat{\mathscr{L}}_\varepsilon u^{j+1}(x) = \varepsilon u_{xx}^{j+1}(x) + a^{j+1}(x)u_x^{j+1}(x) - (b^{j+1}(x) + \frac{1}{k})u^{j+1}(x).$$

Lemma 4 (Minimum principle for time semi-discretization). *Suppose $F^{j+1}(x)$ be smooth function satisfying $F^{j+1}(0) \ge 0, F^{j+1}(1) \ge 0$ and $\hat{\mathscr{L}}_\varepsilon F^{j+1}(x) \le 0, \;\; \forall x \in \ominus$. Then $F^{j+1}(x) \ge 0, \;\; \forall x \in \bar{\ominus}$ and $j = 0,1,2,\ldots,M-1$.*

Proof. let $\ell \in \ominus$ such that $F^{j+1}(\ell) = \min F^{j+1}(x) < 0, \;\; \forall x \in \ominus$, which implies that $(F^{j+1}(\ell))' = 0$ and $(F^{j+1}(\ell))'' \ge 0$. Then, we have

$$\hat{\mathscr{L}}_\varepsilon F^{j+1}(\ell) = \frac{\varepsilon}{2}(F^{j+1}(\ell))'' + \frac{a^{j+1}(x)}{2}(F^{j+1}(\ell))' - \frac{c^{j+1}(x)}{2}(F^{j+1}(\ell)) > 0,$$

since $c^{j+1}(\ell) = b^{j+1}(\ell) + \frac{2}{k} \ge \beta + \frac{2}{k} > 0$. This contradict the assumption that $\hat{\mathscr{L}}_\varepsilon F^{j+1}(x) \le 0$. Therefore, $F^{j+1}(x) \ge 0$ on $\bar{W}$. □

Lemma 5. *If $u^{j+1}(0) \ge 0$ and $u^{j+1}(1) \ge 0$, then*

$$\left|u^{j+1}(x)\right| \le \max\{u^{j+1}(0), u^{j+1}(1)\} + \max_{x \in D} \frac{|\hat{\mathscr{L}}_\varepsilon u^{j+1}(x)|}{\beta}.$$

Proof. The proof is similar to the proof in [5]. □

The local error of the time semi-discretization method (9) is given by $e_{j+1} \equiv u(x,t_{j+1}) - \hat{u}^{j+1}(x)$, where $\hat{u}^{j+1}(x)$ is the solution of

$$\begin{cases} \hat{\mathscr{L}}_\varepsilon \hat{u}^{j+1}(x) = f^{j+1}(x) - \frac{u^j(x)}{k}, \\ \hat{u}(0,t_{j+1}) = \phi(t_{j+1}), \hat{u}(1,t_{j+1}) = \psi(t_{j+1}), \hat{u}(x,0) = u_0(x), 0 < x < 1. \end{cases} \tag{11}$$

Theorem 2. *Suppose that*

$$\left|\frac{\partial^i u}{\partial t^i}\right| \le C, \;\; (x,t) \in \bar{W} \;\; for \;\; 0 \le i \le 2.$$

The local truncation error at $(j+1)^{th}$ time step is given by $|e_{j+1}| \le Ck^2$.

Proof. Using Taylor series expansion, we have

$$u(x,t_{j+1}) = u(x,t_j) + ku_t(x,t_j) + O(k^2). \tag{12}$$

Then

$$\begin{aligned} \frac{u(x,t_{j+1}) - u(x,t_j)}{k} &= u_t(x,t_j) + O(k) \\ &= \varepsilon(u_{xx})^{j+1} + (a(x)^{j+1}(u_x)^{j+1} - (b(x))^{j+1}(u(x))^{j+1} - f^{j+1}(x) + O(k). \end{aligned}$$

Now, it can be seen that the local error is the solution of

$$\hat{\mathscr{L}}_\varepsilon e_{j+1} = O(k^2),$$
$$e_{j+1}(0) = e_{j+1}(1) = 0.$$

Then, Lemma 5 gives the required result. □

The local error estimate of each time step contributes to the global error in the temporal semi-discretization which is defined, at t_j, as $E_j = u(x,t_j) - u^j(x)$.

Theorem 3. *The global truncation error for temporal discretization up to j^{th} time level is given by*

$$||E_j|| \leq Ck, \quad \forall j \leq \frac{T}{k}.$$

Proof. Using the local error estimate up to j^{th} time step, we obtain the global error estimate at j^{th} time step as follows:

$$\begin{aligned} ||E_j|| &= ||\sum_{i=1}^{j} e_i|| \qquad (j \leq \frac{T}{k}) \\ &\leq ||e_1|| + ||e_2|| + ||e_3|| + \cdots + ||e_j|| \\ &\leq C_1(jk).k \\ &\leq C_1 T(k) \qquad (Since \quad jk \leq T) \\ &\leq Ck, \quad C = C_1 T. \end{aligned}$$

□

3.2 Spatial semi-discretization

For the spatial derivative approximations, the procedures of non-standard finite difference approximations stated in [14] are used. The spatial domain $\bar{\ominus} = [0,1]$ is discretized using uniform space length h as

$$\bar{\ominus}^N = \left\{ x_i = ih, \quad i = 1,\ldots,N-1, x_0 = 0, x_N = 1, \quad h = \frac{1}{N} \right\}, \tag{13}$$

where N is the number of mesh intervals in the spatial discretization. Now, consider (10) using the lower bounds of the coefficients and the homogeneous part

$$\varepsilon u_{xx} + \alpha u_x - \beta u = 0. \tag{14}$$

$$\varepsilon u_{xx} + \alpha u_x = 0. \tag{15}$$

According to [1], the layer behavior of (14) and (15) are the same. The finite difference scheme that replaced h^2 by a non-negative denominator function ξ^2 is

$$\varepsilon \frac{U_{i+1} - 2U_i + U_{i-1}}{\xi_i^2} + a\frac{U_{i+1} - U_i}{h} = 0. \tag{16}$$

We can find ξ_i^2 using the following procedures. First, we rewrite equation (15) equivalently as a first-order coupled system of differential equations

$$\frac{du}{dx} = y, \tag{17}$$

$$\frac{dy}{dx} = \frac{-\alpha}{\varepsilon} y. \tag{18}$$

From (18) we have $y(x) = \exp(-\frac{\alpha}{\varepsilon}x)$. By applying the first order difference scheme for (17) as

$$y_i = \frac{U_{i+1} - U_i}{h} = \exp(-\frac{\alpha}{\varepsilon}x_i), \tag{19}$$

and then substituting (19) into (16), we obtain the denominator function $\xi_i^2 = \frac{h\varepsilon}{\alpha}(\exp(\frac{h\alpha}{\varepsilon}) - 1) \equiv h^2 + O(\frac{h^3}{\varepsilon})$. So (16) becomes

$$\varepsilon \frac{(U_{i+1} - 2U_i + U_{i-1})}{\frac{h\varepsilon}{\alpha}(\exp(\frac{h\alpha}{\varepsilon}) - 1)} + \alpha \frac{(U_{i+1} - U_i)}{h} = 0.$$

Therefore, h^2 can be replaced by the denominator function $\xi^2 = \frac{h\varepsilon}{\alpha}(\exp(\frac{h\alpha}{\varepsilon}) - 1)$.

Adopt this denominator function to the variable coefficient problem written as

$$\xi_{i,j+1}^2 = \frac{h\varepsilon}{a_i^{j+1}}(\exp(\frac{ha_i^{j+1}}{\varepsilon}) - 1), \tag{20}$$

where $\xi_{i,j+1}^2$ is a function of ε, h *and* $a_i^{j+1} = a(x_i, t_{j+1})$. Using (10) and (20), the full discrete scheme is

$$\begin{aligned} \hat{\mathscr{K}}_\varepsilon^N U^{j+1}(x_i) &\equiv \varepsilon \frac{(U_{i+1}^{j+1} - 2U_i^{j+1} + U_{i-1}^{j+1})}{\xi_{i,j+1}^2} + a_i^{j+1} \frac{(U_{i+1}^{j+1} - U_i^{j+1})}{h} - (b_i^{j+1} + \frac{1}{k}) U_i^{j+1} \\ &= f_i^{j+1} - \frac{U_i^j}{k}, \end{aligned} \tag{21}$$

$$u_0^{j+1} = \phi(t_{j+1}), \quad u_N^{j+1} = \psi(t_{j+1}), \quad u_i^0 = u_0(x_i), \quad i = 1,2,3,\ldots,N-1, \quad j = 0,1,2,\ldots,M-1,$$

After rearranging the terms in (21), we arrive at the following recurrence relation

$$r_i^- U_{i-1}^{j+1} + r_i^c U_i^{j+1} + r_i^+ U_{i+1}^{j+1} = H_i^j, \tag{22}$$

where the coefficients are given by

$$\begin{cases} r_i^- = \dfrac{\varepsilon}{\xi_{i,j+1}^2}, \\ r_i^c = -(\dfrac{2\varepsilon}{\xi_{i,j+1}^2} + \dfrac{a_i^{j+1}}{h} + b_i^{j+1} + \frac{1}{k}), \\ r_i^+ = \dfrac{\varepsilon}{\xi_{i,j+1}^2} + \dfrac{a_i^{j+1}}{h}, \\ H_i^j = f_i^{j+1} - \dfrac{U_i^j}{k}. \end{cases}$$

Since $|r_i^c| \geq |r_i^-| + |r_i^+|$, the tri-diagonal system (22) is diagonally dominant system of equations. So it has a unique solution. Thus, we can use any tri-diagonal solver, such as Thomas algorithm, to solve this system of equations.

4 Stability and convergence analysis

In this section, we study the discrete minimum principle, stability and $\varepsilon-$uniform convergence for the scheme (21).

Lemma 6 (The discrete minimum principle). *Assume that* $U_0^{j+1} \geq 0, U_N^{j+1} \geq 0$ *and* $\hat{\mathscr{L}}_\varepsilon^N U_i^{j+1} \leq 0$ *for* $0 < i < N, 0 \leq j < M$. *Then,* $U_i^{j+1} \geq 0$ *for* $0 < i < N, 0 \leq j < M$.

Proof. Suppose there exists $s \in \{0,1,2,\ldots,N\}$ such that $U_s^{j+1} = \min\limits_{0\leq i\leq N} U_i^{j+1} < 0$ which implies $k \neq 0$ and $k \neq N$. Also we have $(U_{s+1}^{j+1} - U_s^{j+1}) > 0$ and $(U_{s-1}^{j+1} - U_s^{j+1}) > 0$. Then

$$\begin{aligned}\mathscr{K}_\varepsilon^N u_s^{j+1} &= \varepsilon \frac{(U_{s+1}^{j+1} - 2U_s^{j+1} + U_{s-1}^{j+1})}{\xi^2} + a_s^{j+1}\frac{(U_{s+1}^{j+1} - U_s^{j+1})}{h} - (b_s^{j+1} + \frac{1}{k})U_s^{j+1} \\ &= \varepsilon \frac{(U_{s+1}^{j+1} - U_s^{j+1}) + (U_{s-1}^{j+1} - U_s^{j+1})}{\xi^2} + a_s^{j+1}\frac{(U_{s+1}^{j+1} - U_s^{j+1})}{h} - (b_s^{j+1} + \frac{1}{k})U_s^{j+1} > 0,\end{aligned}$$

since $(b_s^{j+1} + \frac{1}{k}) > \beta > 0$. It contradict the assumption that $\hat{\mathscr{K}}_\varepsilon^N U_i^{j+1} \leq 0$ *for* $0 < i < N, 0 \leq j < M$. Therefore, the operator $\hat{\mathscr{K}}_\varepsilon^N$ satisfies the discrete minimum principle. □

Lemma 7. *The solution of the discrete problem* (21) *satisfies the bound*

$$\left|u_i^{j+1}\right| \leq \left|\left|\hat{\mathscr{L}}_\varepsilon{}^N u_i^{j+1}\right|\right| + \max(|\psi(t_{j+1})|, |\phi(t_j{+}1)|).$$

Proof. Consider the barrier function

$$\psi^\pm(x_i, t_{j+1}) = \left|\left|\hat{\mathscr{L}}_\varepsilon{}^N u_i^{j+1}\right|\right| + \max(|\psi(t_{j+1})|, |\phi(t_{j+1})|) \pm u_i^{j+1}.$$

At the boundary points we have

$$\begin{aligned}\psi^\pm(0, t_{j+1}) &= \left|\left|\hat{\mathscr{L}}_\varepsilon{}^N u_0^{j+1}\right|\right| + \max(|\psi(t_{j+1})|, |\phi(t_{j+1})|) \pm u_0^{j+1} \geq 0, \\ \psi^\pm(1, t_{j+1}) &= \left|\left|\hat{\mathscr{L}}_\varepsilon{}^N u_N^{j+1}\right|\right| + \max(|\psi(t_{j+1})|, |\phi(t_{j+1})|) \pm u_N^{j+1} \geq 0.\end{aligned}$$

For the interior points we have

$$\begin{aligned}\hat{\mathscr{L}}_\varepsilon{}^N \psi_{i,j+1}^\pm &= \varepsilon\delta_x^2 \psi_{i,j+1}^\pm + a_i^{j+1} D_x^+ \psi_{i,j+1}^\pm - (b_i^{j+1} + \frac{1}{k})\psi_{i,j+1}^\pm \\ &= \varepsilon\delta_x^2 \psi_{i,j+1}^\pm + a_i^{j+1} D_x^+ \psi_{i,j+1}^\pm - (b_i^{j+1} + \frac{1}{k})(\left|\left|\hat{\mathscr{L}}_\varepsilon{}^N u_i^{j+1}\right|\right| + \max(|\psi(t_{j+1})|, |\phi(t_{j+1})|) \pm u_i^{j+1}) \\ &= -(b_i^{j+1} + \frac{1}{k})(\left|\left|\hat{\mathscr{L}}_\varepsilon{}^N u_i^{j+1}\right|\right| + \max(|\psi(t_{j+1})|, |\phi(t_{j+1})|)) \pm \hat{\mathscr{L}}_\varepsilon{}^N u_i^{j+1} \\ &\leq 0.\end{aligned}$$

Now, using Lemma 6, we get the desired result. □

Lemma 8. *For $\varepsilon \to 0$ and fixed mesh, the following holds*

$$\lim_{\varepsilon\to 0} \frac{\exp(-x_i\sqrt{(\beta/\varepsilon)})}{(\sqrt{\varepsilon})^s} = 0, \;\; s \in Z^+.$$

Proof. We have

$$\frac{\exp(-x_i\sqrt{(\beta/\varepsilon)})}{(\sqrt{\varepsilon})^s} \le \frac{\exp(-x_1\sqrt{(\beta/\varepsilon)})}{(\sqrt{\varepsilon})^s} = \frac{\exp(-h\sqrt{(\beta/\varepsilon)})}{(\sqrt{\varepsilon})^s} \;\; for \;\; i = 1,2,\ldots,N.$$

Let $\eta = 1/\sqrt{\varepsilon}$, then

$$\lim_{\varepsilon\to 0} \frac{\exp(-h\sqrt{(\beta/\varepsilon)})}{(\sqrt{\varepsilon})^s} = \lim_{\eta\to\infty} \frac{\eta^s}{\exp(h\sqrt{\beta}\eta)}.$$

Applying L'Hospital's rule repeatedly, we have

$$\lim_{\varepsilon\to 0} \frac{\exp(-h\sqrt{(\beta/\varepsilon)})}{(\sqrt{\varepsilon})^s} = \lim_{\eta\to\infty} \frac{\eta^s}{\exp(h\sqrt{\beta}\eta)} = \lim_{\eta\to\infty} \frac{s!}{(h\sqrt{\beta})^s \exp(h\sqrt{\beta}\eta)} = 0. \qquad \square$$

Theorem 4. *Let $U^{j+1}(x_i)$ and U_i^{j+1} be the exact solution of (1) and the numerical solution of (21), respectively. Then, the proposed scheme satisfies the following error bound at $(j+1)^{th}$ time level;*

$$\left|u^{j+1}(x_i) - U_i^{j+1}\right| \le CN^{-1}.$$

Proof. The truncation error in the spatial discretization is

$$\begin{aligned}\left|\hat{\mathscr{L}_\varepsilon}^N(U^{j+1}(x_i) - U_i^{j+1})\right| &= \left|(\hat{\mathscr{L}_\varepsilon}U^{j+1}(x_i) - \hat{\mathscr{L}_\varepsilon}^N U_i^{j+1})\right| \\ &\le \left|\varepsilon(\frac{d^2}{dx^2} - \delta_x^2)U_i^{j+1} + a_i^{j+1}(\frac{d}{dx} - D^+)U_i^{j+1}\right|,\end{aligned}$$

where

$$\delta_x^2 U_i^{j+1} = \frac{U_{i+1}^{j+1} - 2U_i^{j+1} + U_{i-1}^{j+1}}{\xi^2} \;\text{ and }\; D_x^+ U_i^{j+1} = \frac{(U_{i+1}^{j+1} - U_i^{j+1})}{h}.$$

Now, using Taylor series expansion of U_{i+1}, U_{i-1}, ξ^2 and bounds on the derivatives of U from Theorem 1 we have the following:

$$\begin{aligned}\left|(\hat{\mathscr{L}_\varepsilon}U^{j+1}(x_i) - \hat{\mathscr{L}_\varepsilon}^N U_i^{j+1})\right| \le \Bigg|&(\varepsilon(1 - \frac{h^2}{\xi^2}) - \frac{ha_i^{j+1}}{2})\frac{d^2U^{j+1}(x_i)}{dx^2} \\ &- a_i^{j+1}\frac{h^2}{6}\frac{d^3U^{j+1}(x_i)}{dx^3} - a_i^{j+1}\frac{\varepsilon h^4}{12\xi^2}\frac{d^4U^{j+1}(x_i)}{dx^4}\Bigg| \\ \le C(&\left|h(1+\varepsilon^{-1}e^{-x_i\sqrt{(\beta/\varepsilon)}})\right| + \left|h^2(1+\varepsilon^{-3/2}e^{-x_i\sqrt{(\beta/\varepsilon)}})\right| \\ &+ \left|\frac{\varepsilon h^4}{\xi^2}(1+\varepsilon^{-2}e^{-x_i\sqrt{(\beta/\varepsilon)}})\right|) \\ \le C(&|h(1+\varepsilon^{-1}e^{-x_i\sqrt{(\beta/\varepsilon)}})| + |h^2(1+\varepsilon^{-3/2}e^{-x_i\sqrt{(\beta/\varepsilon)}})| \\ &+ |h^3(1+\varepsilon^{-2}e^{-x_i\sqrt{(\beta/\varepsilon)}})|).\end{aligned}$$

Since $h^3 < h^2 < h$ and using Lemma 7 and 8, we have $\left|(U^{j+1}(x_i) - U_i^{j+1})\right| \le CN^{-1}$. $\square$

Theorem 5. *The solution U_i^{j+1} of the fully discrete scheme (21) converges uniformly to the solution $u(x,t)$ of (1) and the error estimate is given by*

$$\sup_{0<\varepsilon\ll 1}\left|u(x_i,t_j)-U_i^{j+1}\right|\leq C(N^{-1}+M^{-1}),\qquad i=0,1,2,\ldots,N,\;\; j=0,1,2,\ldots,M.$$

Proof. The uniform convergence of the scheme follows from the Theorems 3 and 4. We justify it as follows:

$$\sup_{0<\varepsilon\ll 1}\left|u(x_i,t_{j+1})-U_i^{j+1}\right|\leq \sup_{0<\varepsilon\ll 1}\left|u(x_i,t_{j+1})-U^{j+1}(x_i)\right|+\sup_{0<\varepsilon\ll 1}\left|U^{j+1}(x_i)-U_i^{j+1}\right|\leq C(N^{-1}+M^{-1}),$$

for $i=0,1,2,\ldots,N$, and $j=0,1,2,\ldots,M$. □

To enhance the order of convergence, we applied the Richardson extrapolation technique as follow. Let $U_{i,j+1}^{2N,2M}$ denote for an approximate solution on $2N$ and $2M$ number of mesh intervals by including the mid point $(x_{i+1/2},t_{j+1/2})$ into the mesh points. Then the extrapolation formula becomes $U_{i,j+1}^{ext}=2U_{i,j+1}^{2N,2M}-U_{i,j+1}^{N,M}$. Thus, the uniform error bound becomes

$$\sup_{0<\varepsilon\ll 1}\left|u(x_i,t_j)-U_{i,j+1}^{ext}\right|\leq C(N^{-2}+M^{-2}),\qquad i=0,1,2,\ldots,N,\;\; j=0,1,2,\ldots,M.$$

5 Numerical results and discussion

In this section, we conduct the numerical experiments on two test problems to validate the theoretical results. The numerical results are also compared with the scheme available in the literature for the considered class of problems to demonstrate the accuracy and acceptance of the proposed scheme.

Example 1. Consider singularly perturbed multiple boundary turning points problem in [7]

$$\begin{aligned}&\varepsilon u_{xx}(x,t)+x^p u_x(x,t)-u(x,t)-u_t(x,t)=x^2-1,\;\;(x,t)\in W,\\&u(x,0)=0,\;\;0\leq x\leq 1,\;\;u(0,t)=t,\;\;u(1,t)=0,\;\;0\leq t\leq 1.\end{aligned}$$

Example 2. Consider singularly perturbed multiple boundary turning points problem in [21]

$$\begin{aligned}&\varepsilon u_{xx}(x,t)+x^p u_x(x,t)-u(x,t)-u_t(x,t)=x^2-1,\;\;(x,t)\in W,\\&u(x,0)=(1-x)^2,\;\;0\leq x\leq 1,\;\;u(0,t)=1+t^2,\;\;u(1,t)=0,\;\;0\leq t\leq 1.\end{aligned}$$

In science and modern life, the convection-diffusion-reaction (CDR) differential equations provide a beneficial, influential, and vital mathematical model. It describes how the concentration of the substance is distributed. When the CDR model is dominated by convection, then it is called singularly perturbed CDR equation. Some numerical methods have been activated to solve them during some decades, and new techniques still draw more attention. In these examples, we assume the diffusion coefficient (viscosity) is small i.e $0<\varepsilon\ll 1$ and the convective coefficient (velocity) is both linear($p=1$) and non-linear ($p>1$) distribution. To propagate the numerical solutions of these initial boundary value problems, we have used MATLAB programming.

For each ε, maximum absolute errors are used to measure the accuracy of the method. Since exact solutions of these two examples are not available, double mesh principle is used to estimate maximum pointwise error before and after extrapolation

$$e_{\varepsilon}^{N,M} = \max_{0\le i,j\le N,M} \left| U^{N,M}(x_i,t_j) - U^{2N,2M}(x_i,t_j) \right|,$$
$$(e_{\varepsilon}^{N,M})^{ext} = \max_{0\le i,j\le N,M} \left| (U^{N,M}(x_i,t_j))^{ext} - (U^{2N,2M}(x_i,t_j))^{ext} \right|,$$

respectively. The rate of convergence is

$$p_{\varepsilon}^{N,M} = \log_2(e_{\varepsilon}^{N,M}/e_{\varepsilon}^{2N,2M}).$$

Furthermore, ε-uniform point-wise error is defined by

$$e^{N,M} = \max_{\varepsilon} e_{\varepsilon}^{N,M},$$

and its corresponding $\varepsilon-$ uniform rate of convergence is

$$p^{N,M} = \log_2(e^{N,M}/e^{2N,2M}).$$

We computed $e^{N,M}$, $e_{\varepsilon}^{N,M}$ and $p^{N,M}$ using the developed scheme (21) for each model example. The results are displayed using tables and figures. The maximum absolute error and their corresponding rate of convergence for Example 1 before and after extrapolation are listed for different values of ε and $N = M$ in Table 1. The numerical results in Table 1 show that the proposed method is $\varepsilon-$uniformly convergent. Moreover, the results confirm that the proposed method has second order convergence after extrapolation. In Table 2, the maximum ε-uniform absolute error and their corresponding order of convergence obtained using the proposed method is compared with the method given in [8, 21] for Example 2 at $p = 1$. From this Table it can be observed that as the mesh parameter increases the proposed method has relatively rapid convergence and better accuracy than the compared methods. In Table 4, the maximum absolute error and their corresponding order of convergence obtained using the proposed method is compared with the method given in [7] for Example 1 at $p = 1$ and $\varepsilon = 2^{-10}$. From the comparison it is observed that the proposed method has better accuracy and order of convergence than the scheme in [7]. The larger errors in [7, 8] are the price it pays for straggling to resolve the boundary layer due to the meshes' design, which is condensed in the boundary layer region. Further, in Table 3, we listed $\varepsilon-$uniform point wise error and their corresponding rate convergence for different values of p for Example 2. From the results we observed that the error estimate does not depend on the values of p. Some numerical approximate values are displayed in Table 5. This Table shows that, when $\varepsilon = 1$ the solution changes smoothly throughout the domain. When $\varepsilon = 10^{-4}$, the solution changes from 1 to 0.5712 for Example 1 and 2 to 0.7303 for Example 2 near the boundary layer $x = 0$. This difference is large compared with the remaining corresponding difference. Therefore, as $\varepsilon \to 0$, the solution shows an abrupt change near the boundary layer $x = 0$. Surface plots for the numerical solution of the proposed method are displayed in Figure 1 and Figure 3 for Example1 and Example 2 respectively. Each Figure reveal that the boundary layer is located on the left side of the spatial domain as $\varepsilon \to 0$. As one observes in Figure 1 and Figure 3 as $\varepsilon \to 0$; the boundary layer formation becomes more visible because of the abrupt change of the solution near $x = 0$. Figure 2 and Figure 4 are plotted for Examples 1 and 2 respectively, at different time levels to show the changes in the boundary layer with respect to the perturbation parameter. As the perturbation parameter ε decreases to zero, the width of the boundary layer also decreases.

Table 1: Maximum absolute error and rate of convergence for Example 1 at $p = 1$.

Before Extrapolation					
$\varepsilon \downarrow M = N \rightarrow$	32	64	128	256	512
2^{-10}	5.7174e-03	3.1358e-03	1.5466e-03	7.1861e-04	3.3495e-04
	0.8665	1.0197	1.1058	1.1013	
2^{-16}	5.7537e-03	3.3039e-03	1.8274e-03	9.8668e-04	5.3477e-04
	0.8003	0.8544	0.8891	0.8837	
2^{-20}	5.7537e-03	3.3039e-03	1.8274e-03	9.8668e-04	5.3477e-04
	0.8003	0.8544	0.8891	0.8837	
$e^{N,M}$	5.7537e-03	3.3039e-03	1.8274e-03	9.8668e-04	5.3477e-04
$p^{N,M}$	0.8003	0.8544	0.8891	0.8837	
After Extrapolation					
2^{-10}	5.3740e-04	1.3582e-04	3.3867e-05	8.0738e-06	1.8407e-06
	1.9843	2.0037	2.0686	2.1330	
2^{-16}	5.3740e-04	1.3584e-04	3.4146e-05	8.5598e-06	2.1429e-06
	1.9841	1.9921	1.9961	1.9980	
2^{-20}	5.3740e-04	1.3584e-04	3.4146e-05	8.5598e-06	2.1429e-06
	1.9841	1.9921	1.9961	1.9980	
$e^{N,M}$	5.3740e-04	1.3584e-04	3.4146e-05	8.5598e-06	2.1429e-06
	1.9841	1.9921	1.9961	1.9980	

Table 2: Comparison of $e^{N,M}$ and $P^{N,M}$ for Example 2 before extrapolation at $p = 1$.

Methods$\downarrow M = N \rightarrow$		32	64	128	256
Proposed Method	$e^{N,M}$	5.0526e-03	2.6737e-03	1.3801e-03	7.0249e-04
	$p^{N,M}$	0.9182	0.9541	0.9742	—
Method in [21]	$e^{N,M}$	8.0607e-03	4.4718e-03	2.4120e-03	1.2744e-03
	$p^{N,M}$	0.8501	0.8906	0.9204	—
Method in [8]	$e^{N,M}$	3.0430e-02	1.1938e-02	6.1610e-03	3.2113e-03
	$p^{N,M}$	1.3499	0.9543	0.9400	—

Table 3: $\varepsilon-$uniform absolute error and rate of convergence for Example 2 before extrapolation for different values of p.

$p \downarrow M = N \rightarrow$	32	64	128	256	512
1	5.0526e-03	2.6737e-03	1.3801e-03	7.0249e-04	3.5479e-04
	0.9182	0.9541	0.9742	0.9855	
2	5.9998e-03	3.2764e-03	1.7260e-03	8.9055e-04	4.5355e-04
	0.8728	0.9247	0.9546	0.9734	
3	6.5480e-03	3.6504e-03	1.9476e-03	1.0138e-03	5.1897e-04
	0.8430	0.9064	0.9419	0.9661	
4	6.8857e-03	3.9140e-03	2.1088e-03	1.1045e-03	5.6777e-04
	0.8149	0.8923	0.9330	0.9600	

Table 4: Comparison of maximum absolute error and rate of convergence for Example 1 before extrapolation for $\varepsilon = 2^{-10}$ with different values of p.

$p \downarrow M = N \rightarrow$	32	64	128	256	512
	Proposed method				
2	6.5814e-03	2.9461e-03	1.2898e-03	5.8669e-04	2.7855e-04
	1.1596	1.1916	1.1365	1.0747	
4	7.0197e-03	3.3075e-03	1.3045e-03	4.2805e-04	2.0726e-04
	1.0856	1.3423	1.6076	1.0464	
6	7.0203e-03	3.3495e-03	1.2431e-03	3.7020e-04	1.7553e-04
	1.0676	1.4300	1.7476	1.0766	
	Method in [7]		.	.	.
2	1.11e-02	5.56e-03	3.07e-03	1.69e-03	8.96e-04
	1.00	0.86	0.86	0.92	
4	1.11e-02	5.59e-03	3.26e-03	1.81e-03	9.60e-04
	0.99	0.78	0.85	0.91	
6	1.11e-02	5.86e-03	3.30e-03	1.81e-03	9.53e-04
	0.92	0.83	0.87	0.93	

Table 5: Numerical solution U_i^{j+1} for $M = N = 8$ and $p = 1$ for a fixed $t = 1$.

Example 1	$\varepsilon = 1$	$\varepsilon = 10^{-2}$	$\varepsilon = 10^{-4}$
$x \downarrow$	$U \rightarrow$		
0	1	1	1
0.125	0.8384	0.5913	0.5712
0.25	0.6898	0.4896	0.4899
0.375	0.5522	0.3840	0.3841
0.5	0.4242	0.2722	0.2722
0.625	0.3049	0.1695	0.1695
0.75	0.1941	0.08658	0.08657
0.875	0.09224	0.02918	0.02918
1	0	0	0

Example 2	$\varepsilon = 1$	$\varepsilon = 10^{-2}$	$\varepsilon = 10^{-4}$
$x \downarrow$	$U \rightarrow$		
0	2	2	2
0.125	1.643	0.8393	0.7803
0.25	1.325	0.5910	0.5891
0.375	1.04	0.4248	0.4246
0.5	0.7852	0.2859	0.2859
0.625	0.5559	0.1731	0.1731
0.75	0.3498	0.08723	0.08723
0.875	0.1649	0.02924	0.02924
1	0	0	0

6 Conclusions

Singularly perturbed convection-diffusion parabolic PDE with boundary turning point problems are considered. The presence of the parameter ε and boundary turning point make the problem stiff. The solution of the considered problem exhibits a left boundary layer on the spatial domain. The solution to this problem at small values of ε has a large oscillatory solution in the boundary layer region. Standard numerical methods on uniform mesh fail to capture the singularly perturbed oscillatory nature of the solution as the perturbation parameter $\varepsilon \rightarrow 0$. To resolve this behaviour of the solution, we developed a numerical scheme using implicit Euler in time and the non-standard finite difference method in space with uniform meshes. The analysis justified that, the scheme is stable and parameter-uniform second-order convergence. The accuracy of the method is not affected by the value of p. The analysis is also

(a) $\varepsilon = 1$ **(b)** $\varepsilon = 2^{-6}$

(c) $\varepsilon = 2^{-12}$ **(d)** $\varepsilon = 2^{-20}$.

Figure 1: Numerical solution profile $(N = M = 64)$ for Example 1 at $p = 1$.

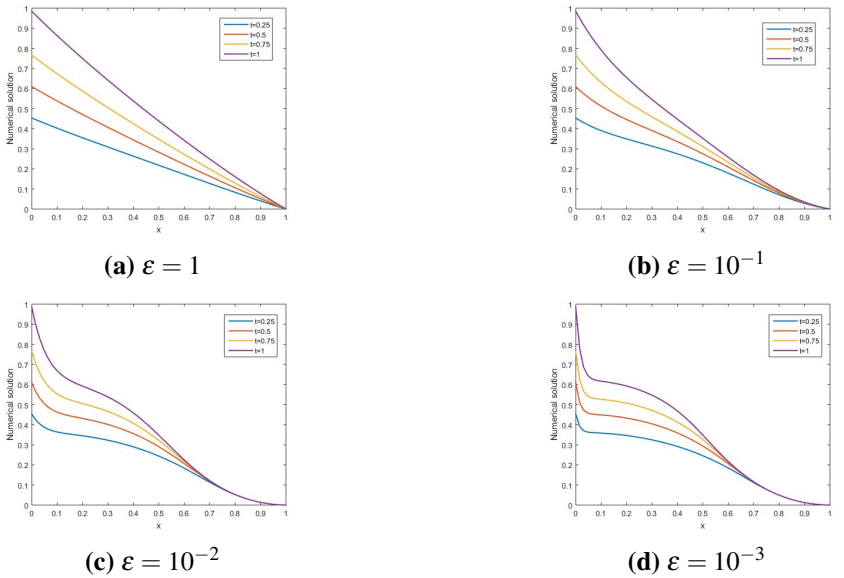

(a) $\varepsilon = 1$ **(b)** $\varepsilon = 10^{-1}$

(c) $\varepsilon = 10^{-2}$ **(d)** $\varepsilon = 10^{-3}$

Figure 2: Numerical solution profile $(M = N = 64)$ for $p = 2$ at different time levels for Example 1.

valid for $p = 0$. The solution behaviour on the perturbation parameter is displayed using Figures and Tables. The surface plot of Example 1 in Figure 1a shows, the solution has uniform behaviour throughout the domain at $\varepsilon = 1$, and Figures 1b-1d show the boundary layer region becomes more evident around $x = 0$ because of the solution's sudden change around that region as $\varepsilon \to 0$. This behaviour is repeated for Example 2 in Figure 3. From Figures 2 and 4, it has been seen that the numerical solution profile for

(a) $\varepsilon = 1$ **(b)** $\varepsilon = 2^{-6}$

(c) $\varepsilon = 2^{-12}$ **(d)** $\varepsilon = 2^{-20}$

Figure 3: Numerical solution profile $(N = M = 64)$ for Example 2 at $p = 2$.

(a) $\varepsilon = 10^{-1}$ **(b)** $\varepsilon = 10^{-3}$

Figure 4: Numerical solution profile $(M = N = 64)$ for $p = 2$ at different time levels for Example 2.

different time levels is close to each other except in the boundary layer region near $x = 0$ and the width of the boundary layer decreases as the singular perturbation parameter $\varepsilon \to 0$. For a fixed singular perturbation parameter $\varepsilon = 2^{-10}$ with different values of p, the maximum absolute error and its corresponding order of convergence in the comparison Table 4 show the proposed method has been found to produce more accurate numerical results. The estimated numerical values of U in Table 5 demonstrate an abrupt change in the solution around $x = 0$ as $\varepsilon \to 0$. The numerical solution of the considered model examples agreed with the theoretical findings. These models are significant examples of singularly perturbed CDR equation that arises in surface mass transport close to the peak of an oceanic rise. The proposed method can be extended to solve singularly perturbed parabolic turning point problems with an interior layer and higher dimensions.

Acknowledgements

The authors wish to appreciate the anonymous referees for their constructive suggestions which have helped to improve the manuscript notably.

References

[1] M.A. Ayele, A.A. Tiruneh, G.A. Derese, *Uniformly convergent scheme for singularly perturbed space delay parabolic differential equation with discontinuous convection coefficient and source term*, J. Math. **2022** (2022) 1874741.

[2] R.K. Dunne, E. ORiordan, G.I. Shishkin, *A Fitted mesh method for a class of singularly perturbed parabolic problems with a boundary turning point*, Comput. Methods Appl. Math. **3** (2003) 361–372.

[3] T.C. Hanks, *Model relating heat-flow values near, and vertical velocities of mass transport beneath, oceanic Rises*, J. Geophys.Res. **76** (1971) 537–544.

[4] Z.I. Hassen, G.F. Duressa, *Nonstandard hybrid numerical scheme for singularly perturbed parabolic differential equations with large delay*, Partial Differ. Equ. Appl. Math. **10** (2024) 100722.

[5] A. Kaushik, N. Sharma, *An adaptive difference scheme for parabolic delay differential equation with discontinuous coefficients and interior layers*, J. Differ. Equ. Appl. **26** (2020) 1450–1470.

[6] R.B. Kellogg, A. Tsan, *Analysis of some difference approximations for a singular perturbation problem without turning points*, Math. Comput. **32** (1976) 1025–1039.

[7] P. Kumari, D. Kumar, H. Ramos, *Parameter independent scheme for singularly perturbed problems including a boundary turning point of multiplicity greater than or equal to one*, J. Appl. Anal. Comput. **13** (2023) 1304–1320.

[8] S. Kumar, Sumit, J. Vigo-Aguiar, *A parameter-uniform grid equidistribution method for singularly perturbed degenerate parabolic convection–diffusion problem*, J. Comput. Appl. Math. **404** (2022) 113273.

[9] H.G. Kumie , A.A. Tiruneh G.A. Derese, *Crank–Nicolson method for solving time-fractional singularly perturbed delay partial differential equations*, Res. Math. **11** (2024) 2293373.

[10] S. Ku Sahoo, V. Gupta, *Second-order parameter-uniform finite difference scheme for singularly perturbed parabolic problem with a boundary turning point*, J. Differ. Equ. Appl. **27** (2021) 223–240.

[11] A. Majumdar, S. Natesan, *An ε-uniform hybrid numerical scheme for a singularly perturbed degenerate parabolic convection–diffusion problem*, Int. J. Comput. Math. **96** (2019) 1313–1334.

[12] A. Majumdar, S. Natesan, *Second-order uniformly convergent Richardson extrapolation method for singularly perturbed degenerate parabolic PDEs*, Int. J. Appl. Comput. Math. **3** (2017) 31–53.

[13] W.G. Melesse, A.A. Tiruneh, G.A. Derese, *Fitted mesh method for singularly perturbed delay differential turning point problems exhibiting twin boundary layers*, J. Appl. Math. Inform. **38** (2020) 113–132.

[14] R.E. Mickens, *Advances in the Applications of Nonstandard Finite Difference Scheme*, World Scientific, 2005.

[15] J.J. H. Miller, E.O. Riordan, *On piece-wise uniform meshes for upwind- and central-difference operators for solving singularly perturbed problems*, IMA J. Numer. Anal. **15** (1995) 89–99.

[16] P. Rai, S. Yadav, *Robust numerical schemes for singularly perturbed delay parabolic convection-diffusion problems with degenerate coefficient*, Int. J. Comput. Math. **98** (2021) 195–221.

[17] S.J. Polak, C. Den Heijer, W.H. A. Schilders, P. Markowich, *Semiconductor device modelling from the numerical point of view*, Int. J. Numer. Methods Eng. **24** (1987) 763–838.

[18] C. Sangeetha, A. Awasthi, *A robust numerical method for solving time dependent singularly perturbed two parameter problem using non-standard finite difference method*, Asian-European J. Math. (2024) 2450084.

[19] K. Sharma, P. Rai, K.C. Patidar, *A review on singularly perturbed differential equations with turning points and interior layers*, Appl. Math. Comput. **219** (2013) 10575–10609.

[20] G.I. Shishkin, *Grid approximations to singularly perturbed parabolic equations with turning points*, Differ. Equ. **37** (2001) 1037–1050.

[21] S.K. Tesfaye, G.F. Duressa, M.M. Woldaregay, T.G. Dinka, *A uniformly convergent numerical scheme for singularly perturbed parabolic turning point problem*, J. Math. Model. **12** (2024) 501–516.

[22] A.A. Tiruneh, G.A. Derese, D.M. Tefera, *A nonstandard fitted operator method for singularly perturbed parabolic reaction-diffusion problems with a large time delay*, Int. J. Math. Math. Sci. **2022** (2022) 5625049.

[23] R. Vulanovic, P.A. Farrell, *Continuous and numerical analysis of a multiple boundary turning point problem*, SIAM J. Numer. Anal. **30** (1993) 1400–1418.

[24] S. Yadav, P. Rai, K. Sharma, *A higher order uniformly convergent method for singularly perturbed parabolic turning point problems*, Numer. Methods Partial Differ. Equ. **36** (2020) 342–368.

[25] A.R. Yaghoubi, H.S. Najafi, *Non-standard finite difference schemes for investigating stability of a mathematical model of virus therapy for cancer*, Appl. Appl. Math. Int. J. **14** (2019) 11.

[26] A.R. Yaghoubi, H.S. Najafi, *A fully implicit non-standard finite difference scheme for one dimensional Burgers' equation*, J. Appl. Res. Ind. Eng. **7** (2020) 301–312.